Determination of Ethanol in Alcohol Samples Using a Modular Raman Spectrometer

ARTICLE *in* JOURNAL OF CHEMICAL EDUCATION · AUGUST 2001

Impact Factor: 1.11 · DOI: 10.1021/ed078p1221

2 AUTHORS, INCLUDING:

Brent A Mantooth
United States Army
36 PUBLICATIONS **1,810** CITATIONS

SEE PROFILE

Topics in Chemical Instrumentation

edited by
David Treichel
Nebraska Wesleyan University
Lincoln, NE 68504

Determination of Ethanol in Alcohol Samples Using a Modular Raman Spectrometer

Caryn L. Sanford* and Brent A. Mantooth
Department of Chemistry, Mercer University, Macon, GA 31207; *seney_cs@mercer.edu

Bradley T. Jones
Department of Chemistry, Wake Forest University, Winston-Salem, NC 27109

An inexpensive Raman spectroscopy system reported in this *Journal* was based on the use of a He–Ne laser and a red-sensitive photomultiplier tube (PMT) (*1*). Another system using the He–Ne laser utilized charge-coupled device (CCD) detection (*2*). With CCD detectors becoming more affordable, they are now more suitable for the undergraduate laboratory experience. The Ocean Optics system (a monochromator with a CCD detector) has the advantage of being not only affordable, but also about 100 times smaller than monochromators with PMT detection; it achieves similar resolution and requires no cooling systems.

Infrared (IR) and Raman spectroscopies are the predominant techniques used by molecular spectroscopists to study the vibrational characteristics of molecular samples. The information extracted by these techniques is often complementary. However, Raman spectrometry has several advantages over IR. For example, measurement of polarization properties of the Raman scattered light can lead to the determination of which of the observed Raman bands result from excitation of the totally symmetric vibrations of the molecule (vibrations that do not cause changes in the symmetry of the molecule). It is also easier to analyze samples in aqueous solution because water is a weak Raman scatterer (*3*). Because Raman spectroscopy has such broad applicability (every molecule exhibits a vibrational Raman spectrum) it is an essential technique to incorporate into the undergraduate curriculum (*4*). Experiments in Raman spectroscopy that have been published in the chemical education literature provide excellent examples of the versatility of this technique (*3*, *5*–*7*).

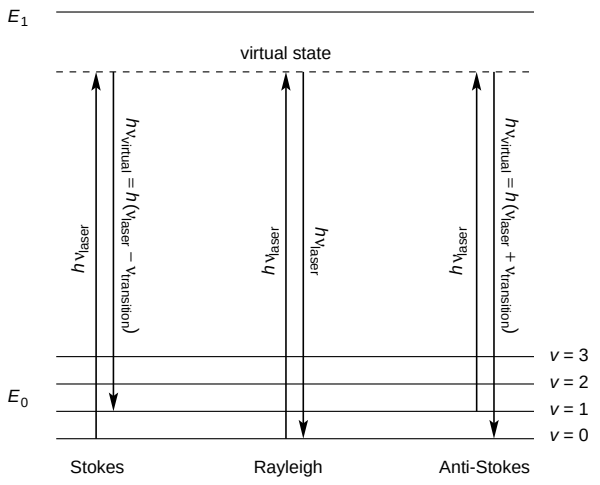

Figure 1. Theory of Raman spectrometry.

Despite exceptional experiments in Raman spectroscopy already described in the chemical literature, Raman is rarely included in the undergraduate laboratory curriculum. Some institutions argue that Raman instrumentation is too complex and expensive to implement in the undergraduate laboratory (*8*). Yet Raman spectrometers are comparable in cost to other analytical instrumentation often purchased by college and university chemistry departments. Moore et al. suggest that the lack of Raman experiments in the laboratory curriculum has resulted from the belief that Raman signals are demonstrably weak, difficult to obtain, or command expensive high-power lasers, optics, and monochromators (*3*).

We describe an inexpensive modular Raman spectrometer that overcomes the cost and the complexity of the traditional equipment while enhancing the pedagogical development of instrumental analysis.

Raman Spectroscopy: Theory

Raman spectra are acquired by irradiating a sample with an intense laser source. During irradiation, the spectrum of scattered light can be measured at 90° and 180° angles with an appropriate spectrometer. The interaction of the laser light with the molecule produces scattering of three types: Stokes, anti-Stokes, and Rayleigh scattering. Scattering involves a momentary distortion of the electrons distributed around a bond in a molecule, followed by re-emission of the radiation as the bond returns to its ground electronic state. The types of scattering are shown in Figure 1, where v is a vibrationally excited state, h is Plank's constant, ν_{laser} is the frequency of the excitation source ($\nu_{laser} = c/\lambda_{laser}$), and $\nu_{transition}$ is the frequency of the photon after interacting with the molecule. A virtual state is an extremely short-lived, excited intermediate energy level that allows radiation of a nonresonant frequency to interact with a molecule. Rayleigh scattering results from the transfer of energy from an incident photon, of energy ($h\nu_{laser}$), to the molecule and the subsequent release of this energy by emission of a photon, of energy ($h\nu_{laser}$), with return of the molecule to the ground state. In Stokes scattering a photon of energy ($h\nu_{laser}$) is transferred to the molecule, promoting it to a virtual state that instantaneously relaxes to a vibrationally excited state [$h(\nu_{laser} - \nu_{transition})$]. Anti-Stokes is similar to Stokes scattering with the exception that a molecule already in a vibrationally excited state interacts with a photon, further exciting the molecule to a higher virtual state followed by relaxation to a lower vibrational level [$h(\nu_{laser} + \nu_{transition})$] (*9*).

The relative population of molecules in the upper vibrational states is low enough that Stokes emission is heavily favored over anti-Stokes scattering. Because the intensity of Raman lines is directly proportional to the Boltzmann distribution and anti-Stokes lines occur at higher frequencies, the anti-Stokes lines have lower populations in the ground state. However, with an increase in temperature the ratio of anti-Stokes to Stokes intensities will increase because a larger fraction of molecules will be in the first vibrationally excited state. Therefore, in some cases the Stokes emission may be favored over anti-Stokes by a factor of 10:1, whereas in other cases it is favored by only 2–3:1. It should also be noted that Rayleigh scattering has a higher probability of occurring than the other types because the most probable event is "absorption" of the radiation by a molecule and subsequent relaxation of this molecule to its original vibrational state, which produces a significantly more intense band than the other two types of scattering. Because the scattered radiation produces a Stokes signal having only 0.0001% of the intensity of the excitation wavelength of the laser (*10*, p 4), detection and measurement of this phenomenon depend on the sensitivity of the detector, intensity of the laser, and concentration and polarizability of the sample. The intensity of Raman-scattered radiation is usually directly proportional to the concentration of the active species. Thus, Raman spectroscopy resembles fluorescence spectroscopy in that the concentration of the analyte is directly proportional to the intensity of the light, whereas in absorption spectroscopy the relationship between concentration and intensity is logarithmic.

Raman spectrometry is often used in conjunction with IR to elicit structural information for inorganic and organic species. However, it is also used to measure physical properties such as certain kinds of equilibrium in solution (particularly acid-dissociation constants), phase transitions, hydrogen-bond strengths, and other quantitative applications (*10*, p 177; *11–13*).

A limitation that threatens the quantitative application of Raman spectroscopy is the possible interference by fluorescence of the sample or impurities within the sample. Many molecular species exhibit fluorescent bands known as Stokes shifts, which are centered at wavelengths longer than the resonance line. As shown in Figure 1, a molecule may be promoted to any of several vibrational levels during the electronic excitation process. However, in solution the excess vibrational energy is lost during collisions between molecules of the excited species and the solvent. This relaxation process is so efficient that on average an excited electronic state is significantly longer lived than the vibrationally excited state that produces Raman scattering. The overlap of fluorescent bands with Raman bands thus occurs in the Stokes spectral region. To overcome the interference from molecules that exhibit fluorescence, one may choose to look at the anti-Stokes bands; however, the intensities of these bands are relatively weak and are often not quantifiable. Another way to eliminate fluorescence is to use a near-IR laser. The increased wavelength of a near-IR laser produces a photon of lower energy than that of visible lasers. Because the energy of the photon is relatively low, it cannot excite a molecule to an electronically excited state; rather, it promotes it to a virtual state, and only a Raman spectrum is produced, thus eliminating the fluorescent interference.

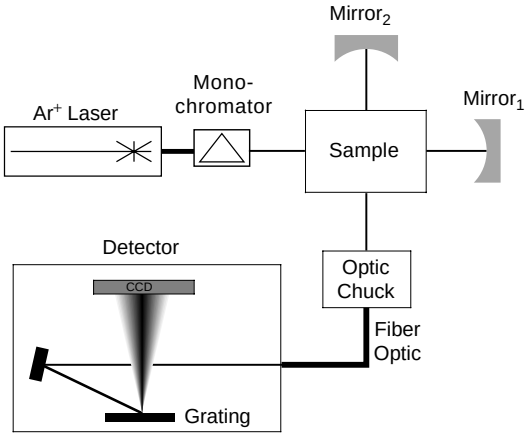

Figure 2. Schematic of Raman spectrometer.

Instrument Design

Figure 2 is a schematic diagram of the instrument. The light source is a Model 532 Omnichrome Air Cooled argon-ion laser operating at 105-mW purchased from Laser Resale for approximately $2000. An Applied Photophysics prism laser filter monochromator (vis), which can be purchased for about $1000, is used to isolate the incident wavelength of 488.0 nm, resulting in a decrease of incident laser intensity estimated at 50-mW. Because the Raman scattering intensity is directly proportional to the incident intensity, a parabolic mirror, mirror$_1$, with a focal length of 12 in. is used to reflect the laser beam through the sample for a second excitation pass. To further enhance the Raman signal a second mirror, mirror$_2$, also a parabolic mirror of focal length 12 in., reflects any back-scatter signal. These parabolic mirrors were stripped from a nonfunctional flame atomic absorption spectrometer. It was determined experimentally that the best signal was generated when both of these mirrors were placed as close as possible to the sample mount. The scattering produced from the laser's interaction with the sample is then collected and focused onto the entrance aperture of a 600-μm fiber optic cable (Fiber Optics Systems, $75) by a fused silica lens located in the "fiber optic chuck". The fiber optic chuck comprises a focusing beam probe, a fused silica lens, and a rod mount for the beam probe, all of which can be acquired from Oriel Corporation for about $260. The opposite end of the fiber optic cable is connected directly to the CCD detector, an Ocean Optics S-2000 CCD detector ($3000) equipped with a 10-μm entrance slit, 600 line/mm grating blazed at 300 nm, and a coated UV array of 1 × 2048 pixels. The detector is controlled by a 90-MHz Pentium computer.

The sample mount was designed and machined from aluminum in house. It is a rectangular box with windows drilled through each of the four faces, allowing the light to pass through the cell. In the center of the cell is a cavity for the placement of a standard four-window 1.000-cm quartz cuvette. Owing to the stability of our design, realignment is not necessary between the analysis of solutions.

The use of a prism monochromator to filter the laser output is optional; however, a wavelength selection device of some type must be used. One option is the use of a holographic notch filter. While a holographic notch filter can be

used to select a narrow bandwidth from the laser, its wavelength selection is static. For this reason, the use of a prism monochromator is beneficial. The monochromator can select any visible wavelength from any source, allowing analysis by several excitation wavelengths with the same wavelength selection device. In the case of our argon ion laser, there are two dominant emissions, 488 and 514 nm. Owing to the nature of Raman scattering, one of these wavelengths can produce a better Raman signal for a given sample than the other can. Thus, the use of a monochromator for wavelength selection allows for the adjustment to any wavelength produced by the laser of choice, providing the potential for a more versatile analysis than a static filter. In addition, if a different laser were used, it would not require its own set of notch filters; it would simply require the adjustment of a wavelength selection device such as the prism monochromator to the proper wavelength. To enhance the signal-to-noise ratio for the peaks at wavenumbers >500, it is common practice to filter the Rayleigh scattering before sending the scattered radiation into a single grating monochromator, thus enabling detection of stretches with 50 (or fewer) wavenumbers of the laser line.

The use of the CCD detector is the greatest benefit of this system (*14*). Its bandwidth of 200–800 nm allows for many types of spectroscopic analysis, including Raman (*2*), fluorescence (*15, 16*), UV–vis (*17*), atomic absorption (*18*), and atomic emission. Moreover, no scanning is required, and an entire spectrum can be obtained in a matter of milliseconds. Another benefit of the S2000 detector is its size (140 × 100 × 35 mm), which includes the grating, CCD detector, and interface electronics. In comparison to a monochromator that uses a PMT (660 × 500 × 200 mm), the S2000 CCD detector is 100 times smaller. Often PMTs require a cooling system to cool the detector to achieve acceptable noise levels; however, the S2000 produces acceptable noise levels at room temperature, making an expensive and bulky cooling system unnecessary. Lastly, the S2000 has a resolution comparable to that reported for more expensive systems that utilize a monochromator with a PMT for detection and exhibit a resolution of 24 cm^{-1}. Each pixel of the CCD represents 10 cm^{-1}, yielding a resolution of 30 cm^{-1}(3 pixels) (*15*). This is indeed a poor resolution for a conventional Raman spectrometer. The spectral bandpass of the current instrument is certainly larger than the typical line width observed for solution Raman spectra. For example, the Raman peak at 3000 cm^{-1} in Figure 4 is in fact a triplet of peaks on either side when measured on a conventional instrument.[1] The peak in Figure 4 appears as a single line with ill-defined shoulders because the resolution of the instrument is insufficient to fully resolve the spectrum.

The components of the instrument are mounted on a 24 × 24-in. bench plate that can be purchased from Edmund Scientific Company for about $490. Overall, as described by the above design, an inexpensive Raman spectrometer has been developed for approximately $10,000 for use in the undergraduate laboratory.

Experimental Procedure (*19*)

Using standard, dehydrated, 200-proof ethanol and deionized water, twenty-two 10-mL standard solutions are prepared within the range of 0 to 100% ethanol (v/v). The samples examined are whiskey, vodka, clear rum, gin, and neutral grain spirits (Everclear). No sample preparation is required. Each sample is analyzed by placing about 1 mL of sample in a standard 4-window, 1.000-cm quartz cuvette. The laser monochromator is set to a wavelength of 488.0 nm, and the spectrometer is set to record spectra with an integration time of 6.659 ± 0.001 s for 10 intervals.

Hazards

Because the laser beam is an extreme vision hazard, proper laser safety goggles for the Ar-ion laser (450–515 nm; may be purchased from MWK Industries) should be used during laser operation, and all guidelines for laser safety should be followed (*http://www.osha-slc.gov:80/OshDoc/Directive_data/PUB_8-1_7.html*).

Results and Discussion

For optimal sensitivity, peak area with baseline correction is calculated to construct the calibration curve (Fig. 3). Each data set is averaged across the last 9 of the 10 intervals; the first is ignored because of a problem inherent in the S2000 software that produces erroneous data for the first interval. The averaged spectra are used for all following spectral calculations. The intensities of the Raman shift −3106 cm^{-1} and −2815 cm^{-1} are averaged to yield a baseline. Each Raman shift from −3096 cm^{-1} to −2825 cm^{-1} is summed after baseline subtraction to produce the peak area used in the calibration curve:

$$\text{area} = \left[\sum_{\nu=-2825\ \text{cm}^{-1}}^{-3096\ \text{cm}^{-1}} \left(\text{intensity}_{\nu} - \frac{\text{intensity}_{-3106\ \text{cm}^{-1}} + \text{intensity}_{-2815\ \text{cm}^{-1}}}{2} \right) \right]$$

The Raman spectra of the 70% ethanol standard and the alcohol samples are represented in Figure 4. Fluorescence is apparent in the gin and whiskey samples as a broad band peak spanning the majority of the spectra. While the peak area method, as described above, attempts to correct for this problem, it does not produce very accurate results. Table 1 summarizes the experimental and theoretical concentrations and the percent difference of ethanol content of the samples as calculated from the calibration curve. The limit of detection as

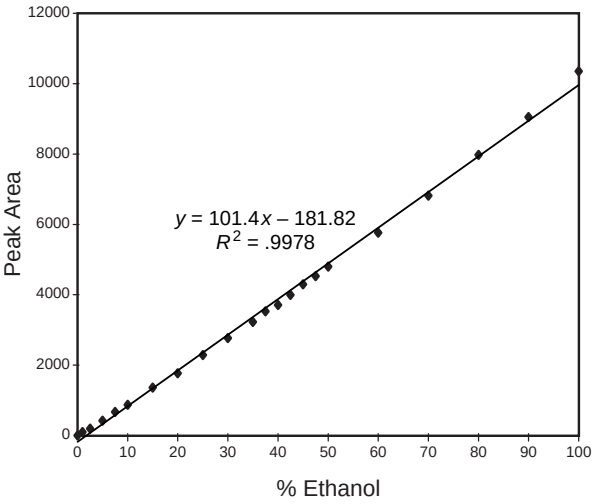

Figure 3. Calibration curve.

Table 1. Data for Ethanol Content of Beverages

Sample	% EtOH		Difference (%)[a]
	Exptl ± σ	Expected	
Vodka	39.4 ± 2.5	40.0	1.46
Everclear	96.6 ± 2.6	95.0	1.63
Rum	39.0 ± 2.3	40.0	2.58
Gin	42.9 ± 2.6	40.0	7.27
Whiskey	52.4 ± 3.9	40.0	31.1

[a]Calculated as $\frac{\text{experimental} - \text{expected}}{\text{expected}} \times 100$, ignoring the sign.

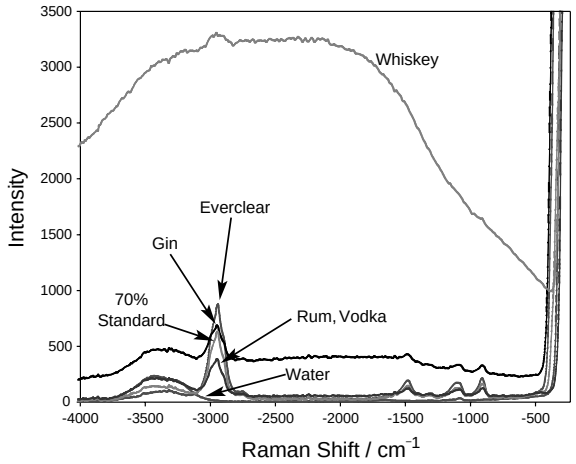

Figure 4. Raman spectra of samples.

calculated by $3\sigma_{blank}/m$, where σ_{blank} is the standard deviation of the peak area of the blank and m is the slope of the calibration curve, is 1% ethanol. To emphasize the linearity of the data, a log–log plot was constructed and the line was well within the limits of linearity; the slope of this plot was 1.03.

The maximum scattering signal occurs at a shift of ~2941 cm^{-1}, indicative of the C–H stretch of ethanol. The use of this peak could be one of the causes for inaccurate results because this peak is characteristic of the C–H stretch of all hydrocarbons, not just ethanol. If other hydrocarbons are present in the sample, they will quantitatively contribute to the intensity of the C–H stretch peak in addition to the scattering of the ethanol. This contribution produces a higher peak area, thereby resulting in a higher than actual experimental value. That the gin and whiskey fluoresced (broad band peak in Fig. 4) but the other samples did not indicates that there are other organic hydrocarbon compounds in the sample. The presence of additional hydrocarbons could explain the positive deviation of the calculated values for ethanol content of the gin and whiskey samples. The fluorescence problem associated with these samples may also result from using the relatively low wavelength (488.0 nm) of the Ar^+ ion laser. Standard deviations of relative peak areas for each concentration for Figure 3 were calculated, and the standard deviations of these concentrations lie between 20 and 30 counts relative peak area.

To improve the signal-to-noise ratio with respect to the instrument, longer detector integration times can be used. However, increasing the integration time will extend the total data acquisition time. For example, if 10 intervals are taken, total data acquisition time is 10 times the integration time. As stated previously, signal-to-noise ratios may also be improved by adding an inexpensive cut-off filter in the area in which the Rayleigh scattering occurs.

Conclusion

The spectrometer was characterized through an analysis of ethanol content in water. Detection limits of 1% ethanol with a 0–100% linear working range for ethanol were determined. Because the system is detector-noise limited, lower detection limits could be achieved by increasing the signal throughput to the detector (increasing the diameter of the fiber optic cable or by increasing the integration time). For the samples that did not fluoresce, the expected alcohol content of the samples corresponded with the calibration curve to within 2.6% of the expected values.

A modular Raman system comparable to those already commercially available, such as the Wizard 1200 by Chromex (*20*) and the Hololab 1000 by Kaiser Optical Systems, Inc. (*21*), has been developed. Our modular design affords comparable spectral resolution and similar spectral range coverage. However, the commercial instruments offer cooled CCD arrays, which greatly enhances the signal-to-noise ratio, thereby reducing the exposure time required. Nevertheless, our research not only demonstrates the feasibility of developing an inexpensive Raman spectrometer, but it also allows students to gain a better practical understanding of analytical instrumentation by permitting them to trace the light path throughout the instrument and observe what occurs to the radiation.

Note

1. Aldrich Spectra Library; Aldrich no. 24511-9, CAS no. 64-17-5.

Literature Cited

1. Fitzwater, D. A.; Thomasson, K. A.; Glinski, R. J. *J. Chem Educ.* **1995,** *72*, 187–189.
2. Pemberton, J. E.; Sobocinski, R. L. *J. Am. Chem. Soc*. **1989,** *111*, 432–434.
3. Moore, R. J.; Trinkle, J. F.; Khandhar, A. J.; Lester, M. I. In *Physical Chemistry. Developing a Dynamic Curriculum*; Schwenz, R. W.; Moore, R. J., Eds.; American Chemical Society: Washington, DC, 1993; pp 217–229.
4. Morris, M. D.; Owen, H. *Am. Lab.* **1996,** *28* (Oct), C21–C23.
5. Aponick, A.; Marchozzi, E.; Johnston, C.; Wigal, C. T. *J. Chem. Educ.* **1998,** *75*, 465–466.
6. Weaver, G. C.; Norrod, K. *J. Chem. Educ.* **1998,** *75*, 621–624.
7. Comstock, M. G.; Gray, J. A. *J. Chem. Educ.* **1999,** *76*, 1272–1275.
8. Galloway, D. B.; Ciolkowski, E. L.; Dallinger, R. F. *J. Chem. Educ.* **1992,** *69*, 79–83.
9. Ingle, J. D. Jr.; Crouch, S. R. *Spectrochemical Analysis*; Prentice Hall: Englewood Cliffs, NJ, 1988; p 499.
10. Long, D. A. *Raman Spectroscopy*; McGraw-Hill International: New York, 1977.
11. Wittkamp, B. L.; Tilotta, D. C. *Anal. Chem.* **1995,** *67*, 600–605.
12. Hill, W.; Rogalla, D. *Anal. Chem.* **1992,** *64*, 2575–2579.

13. Vickers, T. J.; Mann, C. K. *Proc. SPIE—the International Society for Optical Engineering* **1995,** *2504*, 310–315.
14. Carrabba, M. M.; Bello, J. M.; Spencer, K. M.; Haas, J. W. III. Echelle Spectroscopy and CCDs, An Ideal Union for Fiber Optic Raman Systems. In Special Publication; Royal Society of Chemistry: Cambridge, UK, 1996; Vol. 194, pp 128–136.
15. O'Reilly, James E. *J. Chem. Educ*. **1975,** *52*, 610–612.
16. Muenter, J. S. *J. Chem. Educ.* **1996,** *73*, 576–580.
17. Ainscough, E. W.; Brodie, A. M. *J. Chem. Educ.* **1990,** *67*, 1070–1071.
18. Sanford, C. L.; Thomas, S. E.; Jones, B. T. *Appl. Spectrom.* **1996,** *50*,174–181.
19. Procedure adapted from Rice, G. W. *J. Chem. Educ*. **1987,** *64*, 1055–1056.
20. Information regarding product specifications can be requested from Chromex at *http://www.chromexinc.com/* (accessed Jun 2001); select "Products", then "Wizard 1200 Educational System", then "250 mm, f/4.0 spectrograph".
21. For product specifications see Kaiser Optical Systems, Inc. at *http://www.kosi.com/products/labsys.html* (accessed Jun 2001).